Journal of
Synchrotron Radiation

ISSN 0909-0495

Received 21 October 2008
Accepted 1 April 2009

Local structure of uncapped and capped InGaN/GaN quantum dots

E. Piskorska-Hommel,[a,b]* Th. Schmidt,[b] M. Siebert,[b] T. Yamaguchi,[b] D. Hommel,[b] J. Falta[b] and J. O. Cross[c]

[a]Institute of Physics, Polish Academy of Sciences, Al. Lotników 32/46, 02668 Warsaw, Poland, [b]Institute of Solid State Physics, University of Bremen, Otto-Hahn-Allee 1, 28359 Bremen, Germany, and [c]Advanced Photon Source, Argonne National Laboratory, Argonne, IL 60439-4860, USA. E-mail: e.piskorska@ifp.uni-bremen.de

The local structure around the indium atoms in uncapped and capped $In_xGa_{1-x}N$ quantum dots has been studied by In *K*-edge extended X-ray absorption fine structure (EXAFS) spectroscopy. The samples were grown by metal organic vapour phase epitaxy. The EXAFS was successfully applied to study the structural properties of buried quantum dots which are not optically active. The analysis revealed that capping the quantum dots with GaN does not affect the bond distances of the In—N and In—Ga, but makes the In—In distance shorter by 0.04 Å.

Keywords: quantum dots; InGaN; X-ray absorption; EXAFS.

1. Introduction

With increasing In concentration, the emission wavelength of light-emitting InGaN quantum wells can be shifted from violet to amber (380–600 nm). Owing to problems with achieving homogeneous InGaN quantum wells at higher In concentrations, no long-wavelength laser diodes have been realised so far, and stimulated emission is limited to wavelengths below about 485 nm. Therefore, InGaN quantum dots (QDs) have become a promising approach to obtaining stimulated emission in the green spectral region. The Stranski–Krastanov (SK) growth mode has been successfully applied to realise free-standing InGaN QDs. Unfortunately, the free-standing QD islands are not stable under high-temperature overgrowth by GaN (Pretorius *et al.*, 2008). This is mainly caused by significantly different bond strengths between the In—In and Ga—N pairs. For that reason the optimized growth temperatures for InGaN and GaN differ by about 300 K. Therefore, the deposition of a GaN capping layer can lead to dissolution of InGaN dots, resulting in the formation of a more or less homogeneous layer with typical properties of a quantum well (Pretorius *et al.*, 2006). Although a novel two-step approach has been developed to grow InGaN nanostructures that are stable during GaN overgrowth, the estimated QD density of about 10^9 cm^{-2} is rather low in that case (Yamaguchi *et al.*, 2006), and further research is needed to find a mechanism for realising dots of higher density that are stable during overgrowth.

In this paper we present extended X-ray absorption fine structure (EXAFS) measurements of interatomic distances in InGaN QDs grown by a different approach. Comparing uncapped (as-grown) InGaN QDs with those capped with GaN, the interdiffusion between the InGaN dots and the GaN capping layer as well as stress-induced structural properties are studied.

The EXAFS technique is well established for investigating random solutions of III–V semiconductors (Mikkelsen & Boyce, 1983). InGaN alloys and quantum wells have been studied using EXAFS as well (Miyajima *et al.*, 2001; O'Donnell *et al.*, 1999, 2002; Kachankov *et al.*, 2006). Respective bond lengths have also been predicted theoretically (Saito & Arakawa, 1999; Takayama *et al.*, 2000). In the present paper, EXAFS has been applied to study In—N, In—Ga and In—In distances to resolve local structural distortions in self-organized $In_xGa_{1-x}N$ QDs. The EXAFS signal provides average information from the volume of the sample under examination. Therefore the local structure around In atoms present in the QD volume as well as in the wetting layer is probed. Indium *K*-edge EXAFS analysis was performed to determine the local structural distortion in uncapped and capped $In_xGa_{1-x}N$ structures. EXAFS can be considered as an alternative method, *e.g.* to transmission electron microscopy, as it provides valuable structural information about QDs on an atomic level in a non-destructive manner.

2. Experimental

The InGaN QDs were grown by metal organic vapour phase epitaxy on (0001) sapphire substrates. Prior to the growth of the QDs, a 2 μm GaN buffer layer was deposited. The thickness of the InGaN layer was about 3.9 nm at an intended In concentration of about 30%. One sample was left uncapped whereas the another one was capped in a two-step process: first, a thin (2–8 nm) GaN layer was grown at the same

temperature as the InGaN QDs in order to prevent indium segregation and desorption; next, GaN was deposited at a slightly higher temperature to improve the structural quality of the cap layer, the total thickness of which was chosen as 25 nm. Details of the growth conditions can be found elsewhere (Yamaguchi *et al.*, 2006).

In the following, the uncapped and capped structures will be referred to as *A* and *B*, respectively. Atomic force microscopy (AFM) measurements for sample *A*, presented in Fig. 1, show QDs with a density of 10^{12} cm^{-2}, at an average height and diameter of 3.8 and 7.8 nm, respectively. The existence of QDs in the uncapped structure was also identified by grazing-incidence X-ray diffraction (Piskorska *et al.*, 2007).

The In *K*-edge EXAFS spectra were measured in fluorescence mode at the Advanced Photon Source, beamline 20 BM, using a Si(111) double-crystal monochromator and a multi-element Ge fluorescence detector.

The EXAFS $\chi(k)$ oscillations were obtained by subtracting the pre-edge background, normalizing to the experimental edge step, and subtracting a smooth atomic background from normalized absorption data using the *Athena* program (http://cars.uchicago.edu/ifeffit). The theoretical scattering amplitudes for In—N, In—In and In—Ga pairs were generated using the *FEFF8* code (Zabinsky *et al.*, 1995). To obtain the In—Ga scattering amplitude, In atoms in the second coordination shell were replaced by Ga. The *FEFF8* calculation was based on the binary InN structure with lattice constants a = 3.54 Å and c = 5.70 Å (Paszkowicz *et al.*, 2003). The *Artemis* program (Ravel & Newville, 2005) was used to analyze the data using a suitable structural model, as outlined in the following. InGaN crystallizes in the wurtzite structure. Two kinds of nearest-neighbour bonds can be distinguished: a longer one along the *c* axis and three shorter ones in the *c* plane. In order to probe these two different distances separately, polarization-dependent X-ray absorption spectroscopy can be applied (Lawniczak-Jablonska *et al.*, 1997; Miyamaga *et al.*, 2007). However, in the present paper, standard X-ray absorption measurements have been performed. The determination of the bond anisotropy by polarization-dependent X-ray absorption spectroscopy is the aim of future investigations. Hence, the average In—N bond length is reported here. The second coordination shell consists of two contributions, one from the In—Ga pair and another from the In—In pair with different distances. The most reasonable fit assumes a model with four nitrogen neighbours of the absorbing In atom in the first coordination shell, and 12 mixed Ga and In atoms in the second shell. In order to combine their contributions, a mixing parameter x was used.

As reference distances, the theoretical In—N, In—Ga and In—In average distances in wurtzite $In_xGa_{1-x}N$ alloys for various compositions were used (Mattila & Zunger, 1999). Mattila & Zunger calculated the bond lengths in a wurtzite $In_xGa_{1-x}N$ random alloy using a valence force field model (Martin, 1970). In this model the total strain is a function of the atomic position (R_j) accounting for the effects of bond stretching and bond bending. The valence force field method predicts a small deviation of the lattice parameter from Vegard's law for $In_xGa_{1-x}N$ random alloys.

3. Results and discussion

The analysis was performed with k ranging from 3 Å^{-1} to 11 Å^{-1} using a Kaiser–Bessel window, and k-weighted with k^3. The EXAFS oscillation $k^3\chi(k)$ for samples *A* and *B* are shown in Fig. 2. Figs. 3(*a*) and 3(*b*) present the best fit results for the modulus of the Fourier transform (FT) and the real part of the EXAFS oscillation structure for the uncapped and the capped InGaN QDs. Two peaks, centred at 1.6 Å and 2.8 Å, were fitted. At the second peak, a characteristic shoulder is observed. The presence of this shoulder is attributed to the contribution of two different distances in the second coordination shell. Owing to the large difference between the Ga—N and In—N bond lengths, the atomic positions are considered to fluctuate from their perfect lattice sites, leading to bond-

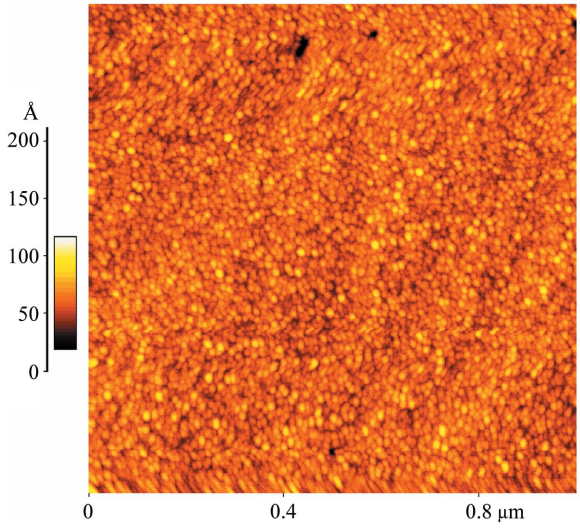

Figure 1
AFM image of uncapped $In_xGa_{1-x}N$ QDs. The density of the dots is about 10^{12} cm^{-2}. Their average height and diameter are 3.8 nm and 7.8 nm, respectively.

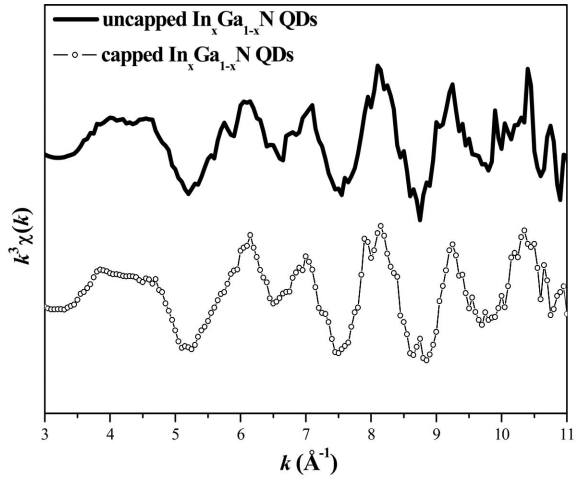

Figure 2
EXAFS $k^3\chi(k)$ oscillations for uncapped (solid line) and capped (dots) $In_xGa_{1-x}N$ QDs.

length distortions and causing a high degree of atomic disorder. In this ternary system, a non-Gaussian distribution is expected owing to the presence of two types of atoms in the second coordination shell. In order to interpret the second-shell EXAFS data, the third and fourth cumulants, which describe the distortion of the radial distribution of atoms in the second shell, were introduced (Bunker, 1983). The third-order cumulant C_3 describes the deviation from the Gaussian shape and the degree of asymmetry of the distribution. Its positive value indicates the presence of a tail on the high-distance r-side of the distribution (Dalba *et al.*, 1993). If the distribution is reversed, the odd cumulants change their signs (Bunker, 1983).

Table 1
Debye–Waller factor (σ^2) and third (C_3) and fourth (C_4) cumulants for the second coordination shell for uncapped and capped structure.

	N	R (Å)	σ^2 (Å^2)	$C_3 \times 10^{-4}$ (Å^3)	$C_4 \times 10^{-14}$ (Å^4)	R-factor
Uncapped sample						
In—N	4	2.09 ± 0.01	0.009 ± 0.001	–	–	0.030
In—Ga	8 ± 1	3.28 ± 0.01	0.025 ± 0.001	9 ± 2	4 ± 1	
In—In	4 ± 1	3.38 ± 0.01	0.031 ± 0.002	−19 ± 2	6 ± 1	
Capped sample						
In—N	4	2.09 ± 0.01	0.008 ± 0.001	–	–	0.033
In—Ga	8 ± 1	3.28 ± 0.01	0.022 ± 0.001	11 ± 1	3 ± 1	
In—In	4 ± 1	3.34 ± 0.02	0.022 ± 0.002	3 ± 3	4 ± 1	

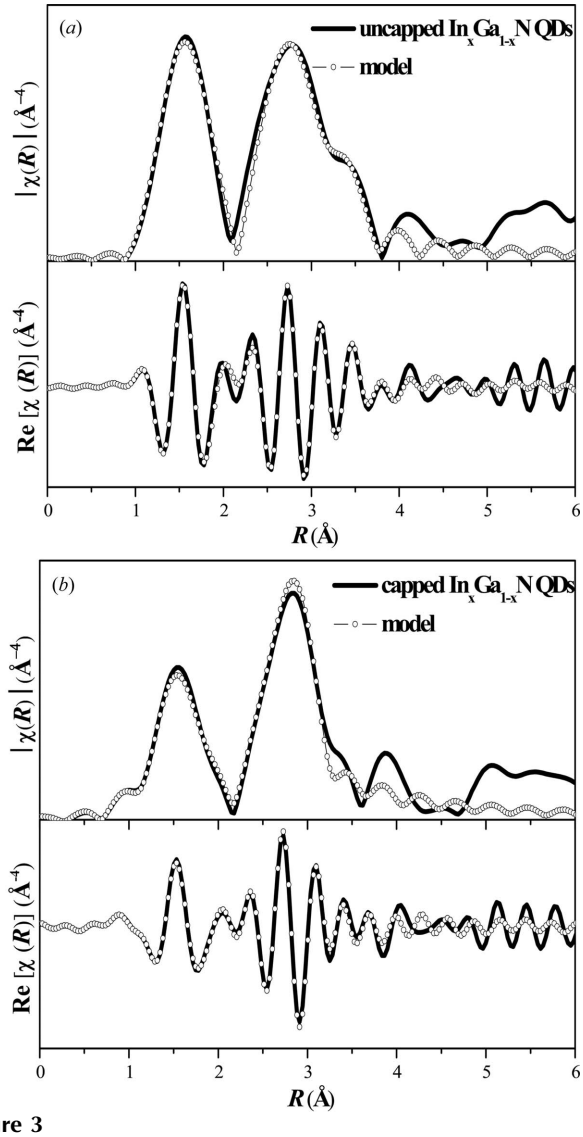

Figure 3
Moduli (top) and real parts (bottom) of the Fourier transforms of the k-weighted EXAFS oscillation collected at the In K-edge. Shown are data (solid line) and the best fit (circles) to the first and second coordination shells in (*a*) uncapped and (*b*) capped $In_xGa_{1-x}N$ QDs. The fitting analysis was carried out in the range R = 1–3.5 Å using a Kaiser–Bessel window.

Since the nearest-neighbour N atoms do not change the positions in the crystal structure, there was no motivation to use the higher-order cumulants for fitting the first shell.

The differences between the FT of the EXAFS oscillations of uncapped and capped QDs, as presented in Figs. 3(*a*) and 3(*b*), are rather small. This indicates that there are no significant changes of the local structures in these two samples. The first peak of the FT corresponds to the average In—N distance. This distance was found to be $R_{In-N} = 2.09 \pm 0.01$ Å for both samples. The In—Ga and In—In distances, which contribute to the second-shell EXAFS, were found to be $R_{In-Ga} = 3.28 \pm 0.01$ Å, $R_{In-In} = 3.38 \pm 0.01$ Å for the uncapped QDs, and, for comparison, $R_{In-Ga} = 3.28 \pm 0.01$ Å and $R_{In-In} = 3.34 \pm 0.02$ Å for the capped QDs. However, the examination of the FTs presented in Figs. 3(*a*) and 3(*b*) shows that the second shell was not split into two subshells. The reason for this is that the difference corresponding to the two distances is too small to be distinguished in separate peaks. Nevertheless, splitting the second shell by assuming two different distances for In—Ga and In—In yielded a significantly improved fit in the numerical analysis.

For sample *A*, the value of the mixing parameter x was found to be $\sim 33 \pm 4\%$ corresponding to eight Ga and four In atoms. For sample *B*, the mixing parameter was found to be slightly lower, $30 \pm 8\%$. The relations between bond lengths and In concentrations obtained from the EXAFS are in good agreement with those predicted by Mattila & Zunger (1999). Therefore, we conclude that the uncapped and capped structures are associated with an $In_xGa_{1-x}N$ random alloy, with $x \simeq 0.3$.

The bond length of the first coordination shell was found to be the same in both samples, and is in the vicinity of the value of 2.15 Å in bulk InN (Miyajima *et al.*, 2001). This result indicates that the In—N bond is similar to that in binary InN. For both samples, the In—Ga bond length in the second coordination shell was found to be the same, 3.28 ± 0.01 Å. However, the second-shell In—In distance was found to be 0.04 Å smaller after capping. We understand this difference as a consequence of the strain introduced by the GaN cap layer, and assume that the Ga atoms remain at their crystal positions, while the In—In distance, owing to stress, is shorter than in the uncapped structure. The strain is caused by the

large mismatch (∼11%) between the lattice constants of GaN and InN.

The EXAFS Debye–Waller factors (σ^2) for the first coordination shell were determined to be 0.009 Å^2 and 0.008 Å^2 for samples *A* and *B*, respectively, suggesting that there are no changes owing to overgrowth. The values of σ^2 for the second coordination shell are presented in Table 1. For the In—Ga distance, σ^2 differs only by about 0.003 Å^2 between the two samples, whereas the difference between this parameter for the In—In path is 0.009 Å^2. As already deduced from the changes of the second-shell distances, the results for the Debye–Waller factor again support the conclusion that only the In—In correlation is affected during overgrowth. It should be noted that the uncapped sample has a large negative value for C_3 of the In—In pair (see Table 1), indicating that the peak distance is fairly longer than 3.38 Å. There is a significant difference in the In—In atomic distance between the capped and uncapped samples, although the average atomic distance shortening is as small as 0.04 Å.

4. Conclusions

EXAFS analysis allows the bond lengths and structural distortions in InGaN QDs to be determined. The cumulants characterizing a deviation from a Gaussian pair distribution applied for the analysis of the second coordination shell significantly improved fitting results. The cumulants used for the analysis of the second coordination shell significantly improved the fitting results being characterized by a deviation from a Gaussian pair distribution. The structural information provided by the EXAFS analysis shows that the GaN capped layer introduces the stress to the studied $In_xGa_{1-x}N$ nanostructure and this effect is pronounced in In—In distances. Remarkably, the mixing parameter x is almost unaffected by cap layer growth. These results indicate that, under the overgrowth conditions chosen here, the structure and composition of the QDs can almost be preserved. It should be pointed out, however, that in the case of sample *B* no photoluminescence from the InGaN QDs could be observed (K. Sebald, private communication). The reason for this might be a still insufficient structural quality of the GaN capping layer, as found by transmission electron microscopy (A. Pretorius, private communication). Therefore, the cap layer growth, which is hampered by the drastically different bond strength of InN as compared with GaN, still needs to be optimized. As shown here, EXAFS provides a non-destructive possibility to study the local structure of such samples and, therefore, might be very helpful to further optimize the capping process.

This work has been supported by a Polish national grant from the Ministry of Science and High Education (No. N202 142 32/3888) and by the German Research Council (Research Group FOR506). The authors would like to thank A. Pretorius, K. Sebald and C. Tessarek for helpful discussions.

References

Bunker, G. (1983). *Nucl. Instrum. Methods*, **207**, 437–444.
Dalba, G., Fornasini, P. & Rocca, F. (1993). *Phys. Rev. B*, **47**, 8502–8514.
Kachankov, V., O'Donnell, K. P., Martin, R. W., Mosselmans, J. F. W. & Pereira, S. (2006). *Appl. Phys Lett.* **89**, 101908.
Lawniczak-Jablonska, K., Suski, T., Liliental-Weber, Z., Gullikson, E. M., Underwood, J. H., Perera, R. C. C. & Drummond, T. J. (1997). *Appl. Phys. Lett.* **70**, 2711–2713.
Martin, R. M. (1970). *Phys. Rev. B*, **1**, 4005–4011.
Mattila, T. & Zunger, A. (1999). *J. Appl. Phys.* **85**, 160–167.
Mikkelsen, C. & Boyce, J. (1983). *Phys. Rev. B*, **28**, 7130–7140.
Miyamaga, T., Azuhata, T., Matsuda, S., Ishikawa, Y., Sasaki, S., Uruga, T., Tanida, H., Chichibu, S. F. & Sota, T. (2007). *Phys. Rev. B*, **76**, 035314.
Miyajima, T., Kudo, Y., Liu, K.-Y., Uruga, T., Asatsuma, T., Hino, T. & Kobayashi, T. (2001). *Phys. Status Solidi B*, **228**, 45–48.
O'Donnell, K. P., Martin, R. W., White, M. E., Mosselmans, J. F. W. & Guo, Q. (1999). *Phys. Status Solidi B*, **216**, 151–156.
O'Donnell, K. P., White, M. E., Pereira, S., Mosselmans, J. F. W., Grandjean, N., Damilano, B. & Massies, J. (2002). *Mater. Sci. Eng. B*, **93**, 150–153.
Paszkowicz, W., Ćerný, R. & Krukowski, S. (2003). *Powder Diffr.* **18**, 114–121.
Piskorska, E., Holy, V., Siebert, M., Krause, B., Schmidt, Th., Falta, J., Yamaguchi, T. & Hommel, D. (2007). *AIP Conf. Proc.* **893** (CD-ROM ISBN: 978–0-7354–0398-7).
Pretorius, A., Yamaguchi, T., Kübel, C., Kröger, R., Hommel, D. & Rosenauer, A. (2006). *Phys. Status Solidi C*, **3**, 1679–1682.
Pretorius, A., Yamaguchi, T., Kübel, C., Kröger, R., Hommel, D. & Rosenauer, A. (2008). *J. Cryst. Growth*, **310**, 748–756.
Ravel, B. & Newville, M. (2005). *J. Synchrotron Rad.* **12**, 537–541.
Saito, T. & Arakawa, Y. (1999). *Phys. Rev. B*, **60**, 1701–1706.
Takayama, T., Yuri, M., Itoh, K., Baba, T. & Harris, J. S. Jr (2000). *J. Appl. Phys.* **88**, 1104–1110.
Yamaguchi, T., Sebald, K., Lohmeyer, H., Gangopadhyay, S., Falta, J., Gutowski, J., Figge, S. & Hommel, D. (2006). *Phys. Status Solidi C*, **3**, 3955–3958.
Zabinsky, S. I., Rehr, J. J., Ankudinov, A., Albers, R. C. & Eller, M. J. (1995). *Phys. Rev. B*, **52**, 2995–3009.